Characterizing a defect in a one-dimensional bar

Cynthia Gangi and Sameer Shah

January 21, 2003

Abstract

We examine the inverse problem of locating and describing an internal point defect in a one-dimensional rod Ω by controlling the heat inputs and measuring the subsequent temperatures at the boundary of Ω. We use a variation of the forward heat equation to model heat flow through Ω, then propose algorithms for locating an internal defect and quantifying the effect the defect has on the heat flow. We implement these algorithms, analyze the stability of the procedures, and provide several computational examples.

1 Introduction

In this paper we study the noninvasive use of thermal energy to detect the presence of a defect in the interior of an object. Specifically, consider a one-dimensional rod Ω which contains a point "defect" in its interior. It is logical to assume that this defect will interfere with the heat flow in Ω. We model the defect as a point "contact resistance," quantified below. One method to determine the defect's location and the nature of its impact on the heat flow is to input a heat flux at both ends of Ω and record the subsequent temperature measurements at these ends for a certain length of time. The presence of a defect, since it alters the heat flow, will manifest itself in the resulting temperature behavior at the endpoints. The goal of this research is to determine if this method of thermal imaging can indeed be employed to successfully find the location and nature of the defect.

This investigation is an extension of the work done by Bryan and Caudill ([1]) on the well-posedness of the forward problem for heat flow in a bar with a point defect under reasonable boundary conditions. The authors demonstrate the existence and uniqueness of classical solutions to this problem. Our research addresses the inverse version of the same problem, in which the goal is to identify internal characteristics (the defect) from boundary data.

The application of inverse problem-solving arises in an area known as *non-destructive testing*, which uses thermal imaging on the surface of an object to locate an internal defect. In other words, by only having knowledge of the boundary of an object, internal blemishes can be characterized without the object's destruction. In our case, it will be shown that merely controlling the boundary heat fluxes of Ω and measuring the resulting boundary temperatures, recovery of the location and nature of a defect is possible.

The inverse problem will be considered in two separate versions– continuous data and finite data. The continuous data version assumes temperature measurements at the endpoints are known for all time while the finite data version assumes that temperature measurements are known for only a finite time interval.

In section 2 we present a mathematical model for the flow of heat through a one-dimensional rod with an interior defect will be presented. The model is an initial-boundary value problem for the heat equation with a component that describes the defect. The defect is modelled as an internal point whose heat flux is governed by the temperature jump at its site rather than the otherwise-applicable heat equation.

Some technical preliminaries are presented in section 3. In section 4, we establish that the location of the defect is uniquely determined by the endpoint temperature measurements and show the recovery of the function defining the defect. Sections 5, 6, and 7 address the finite data version of the recovery of the location of the defect and the function describing it. We discuss the concept of ill-posedness and how to mitigate this phenomenon, along with providing examples of reconstructions, in section 8. Lastly we present a conclusion in section 9.

2 The Forward Problem

Consider a one-dimensional rod Ω spanning an interval $(0, d)$. We use x for spatial position, t for time, and $u(t, x)$ for the temperature of the bar at position x and time t. We assume the interior of the object contains a defect at $x = \sigma$, $0 < \sigma < d$, which impedes the flow of heat in the rod, as quantified below.

Away from the defect we assume that heat flow is modeled by the usual heat equation $\frac{\partial u}{\partial t} - \kappa \frac{\partial^2 u}{\partial x^2} = 0$, where κ is the thermal diffusivity of the bar material (assumed constant in space and time). At the boundaries $x = 0$ and $x = d$ we use Neumann boundary conditions $-\alpha u_x(t, 0) = g_0(t)$ and $\alpha u_x(t, d) = g_1(t)$, where g_0 and g_1 represent the rate at which heat energy is input at the respective ends of the bar and α is the thermal conductivity of the bar. We can rescale by using dimensionless independent variables $\bar{x} = x/d$ and $\bar{t} = t\kappa/d^2$, and define a rescaled temperature function $\bar{u}(\bar{t}, \bar{x}) = u(t, x)$. The function $\bar{u}$ satisfies the heat equation $\frac{\partial \bar{u}}{\partial \bar{t}} - \frac{\partial^2 \bar{u}}{\partial \bar{x}^2} = 0$ for $0 < \bar{x} < 1$ away from $\bar{x} = \sigma/d$, with boundary conditions $-\bar{u}_{\bar{x}}(t, 0) = \bar{g}_0(t)$ and $\bar{u}_{\bar{x}}(t, 1) = \bar{g}_1(t)$ where $\bar{g}_i(t) = \frac{g_i(t)}{\alpha d}$. We will henceforth assume that this rescaling has been done, and simply drop the bars over the variables.

We model the defect as a "contact resistance" to heat flow between the regions on both sides of $x = \sigma$ that causes a temperature jump at $x = \sigma$, as follows. First, we assume that $u_x(t, x)$ (which is proportional to the heat flux through the bar), is continuous across $x = \sigma$ so that the point σ does not store energy. Define $[u](t) = \lim_{x \to \sigma^+} u(t, x) - \lim_{x \to \sigma^-} u(t, x)$, the temperature jump at $x = \sigma$. We model the defect's presence as $u_x(t, \sigma) = F([u](t))$, where F is a non-decreasing, Lipschitz continuous function with $F(0) = 0$. The function F governs how the heat flux and temperature jump over the defect are related, with $F \equiv 0$ modelling a perfectly insulating defect (which completely block the flow of heat).

All in all we find that $u(t, x)$ (after the above-mentioned scaling) satisfies the initial-boundary value problem

$$
\begin{aligned}
u_t(t, x) - u_{xx}(t, x) &= 0 \text{ for } x \in (0, \sigma) \cup (\sigma, 1),\ t > 0 && (1)\\
-u_x(t, 0) &= g_0(t) && (2)\\
u_x(t, 1) &= g_1(t) && (3)\\
u_x(t, \sigma) &= F([u](t)) && (4)\\
u(0, x) &= f(x) && (5)
\end{aligned}
$$

with u_x continuous through $x = \sigma$, where $f(x)$ denotes the initial temperature of the region and $g_0(t), g_1(t)$ the input heat fluxes at $x = 0$ and $x = 1$, respectively. It was proved in [1] that this forward problem is well-posed, and there exists a unique solution which is in $C^1[0, \sigma]$ and $C^1[\sigma, 1]$ for all $t > 0$.

Some simplifying assumptions can be made. In general, we will assume that the initial condition is $f(x) = 0$. Also, we will generally assume that $g_0(t)$ and $g_1(t)$ are piecewise continuous and supported for $t \leq R$ for some positive constant R, so the input fluxes are of finite duration in time.

As mentioned above, we take F to be non-decreasing with $F(0) = 0$. The reasoning for this is as follows: Heat flows in proportion to the temperature gradient, from a region of higher temperature to a region of lower temperature. Since F describes the heat flow across the defect in terms of the

temperature jump, when the temperature difference at the defect is positive (the temperature to the immediate right of the defect is greater than the temperature to its immediate left), the heat flow will be to the left (since heat flows in the direction of $-u_x$). We expect that the greater the jump is at the defect, the greater the heat flow will be through it. Thus F is non-decreasing (and in practice, strictly increasing). Furthermore, if there is no temperature difference at the defect, heat will not flow through it, and thus $F(0) = 0$.

In addition, the following assumptions are made:

A1. The input fluxes g_0 and g_1 are not both identically zero, and the total input energy is finite, so $\int_0^\infty g_0(t)dt < \infty$ and $\int_0^\infty g_1(t)dt < \infty$.

A2. F is uniformly Lipschitz continuous on any bounded interval, i.e. for any $a > 0$ we have $|F(x) - F(y)| \leq C(a)|x - y|$ for $|x|, |y| < a$ and some constant $C(a)$.

A3. We have $xF(x) \geq kx^2$ for some constant $k > 0$ and all x in some neighborhood of zero (so, e.g., the tangent line to $y = F(x)$ at $x = 0$ has positive slope if F is differentiable at $x = 0$).

3 Preliminaries

In this section we note two results that will be useful in the following sections.

Theorem 3.1 *Let $u_1(t, x)$ and $u_2(t, x)$ be solutions to the heat equation for $t_1 < t < t_2$ and $0 < x < c$, continuously differentiable for $x \in [0, c]$, with $u_1(t, 0) \equiv u_2(t, 0)$ and $\frac{\partial u_1}{\partial x}(t, 0) \equiv \frac{\partial u_2}{\partial x}(t, 0)$ for $t_1 < t < t_2$. Then $u_1(t, x) \equiv u_2(t, x)$ for $t_1 < t < t_2$ and $0 < x < c$.*

This is a direct consequence of Theorem 11.4.1 in [2].

Throughout the rest of the paper we will, for simplicity, take the initial condition for Ω as $f(x) = 0$. The validity of this can be ascertained by showing that after a long period of time, the solution to the boundary value problem (1)-(5) will decay to a constant, as quantified by Theorem 3.2 below. This temperature can then be re-scaled to zero, thus giving zero initial conditions to the bar. This result will also be useful for later error analysis.

Theorem 3.2 *Let $u(t, x)$ satisfy the heat equation on $(0, \sigma) \cup (\sigma, 1)$ with zero flux boundary conditions at $x = 0$ and $x = 1$, $u(0, x) = f(x)$ and jump condition $u_x(t, \sigma) = F([u](t))$, where F satisfies the assumptions specified in the previous section. Then,*

$$\int_0^1 (u(t, x) - c)^2 dx \leq Ce^{-2kt/(4k+1)}$$

for some constants C, c, and $k > 0$.

Proof. Let $c = \int_0^1 f(x)dx$ and $v(t, x) = u(t, x) - c$, so $v(t, x)$ satisfies the heat equation on $(0, \sigma) \cup (\sigma, 1)$ with zero flux boundary conditions at $x = 0$ and $x = 1$, $v(0, x) = f(x) - c$, and jump condition $v_x(t, \sigma) = F([v](t))$.

We can compute, using integration by parts, the fact that v satisfies the heat equation, and the zero flux boundary conditions, that

$$\begin{aligned} \frac{\partial}{\partial t}\left(\frac{1}{2}\int_0^\sigma v^2(t, x)dx\right) &= v^-(t, \sigma)v_x(t, \sigma) - \int_0^\sigma v_x^2(t, y)dy \\ \frac{\partial}{\partial t}\left(\frac{1}{2}\int_\sigma^1 v^2(t, x)dx\right) &= -v^+(t, \sigma)v_x(t, \sigma) - \int_\sigma^1 v_x^2(t, y)dy \end{aligned}$$

Adding these two equations yields

$$\frac{\partial}{\partial t}\left(\frac{1}{2}\int_0^1 v^2(t, x)dx\right) = -F([v](t))[v](t) - \int_0^1 v_x^2(t, y)dy. \tag{6}$$

To find a bound for $v(t,x)$ itself, let x_0 be a point in $(0,\sigma)$. We find for any $x \in (0,\sigma)$

$$\begin{aligned} |v(t,x)| &= \left| \int_{x_0}^{x} v_x(t,y)dy + v(t,x_0) \right| \\ &\leq \sqrt{|x-x_0|} \left(\int_0^{\sigma} v_x^2(t,y)dy \right)^{1/2} + |v(t,x_0)| \\ &\leq \left(\int_0^{1} v_x^2(t,y)dy \right)^{1/2} + |v(t,x_0)| \end{aligned} \tag{7}$$

where we have used Hölder's inequality, $\int fg \leq (\int f^2)^{1/2}(\int g^2)^{1/2}$, with $g \equiv 1$. If $x \in (\sigma,1)$ (but still the same $x_0 \in (0,\sigma)$) we find that

$$\begin{aligned} |v(t,x)| &= \left| v^-(t,\sigma) + [v](t) + \int_{\sigma}^{x} v_x(t,y)dy \right| \\ &\leq \left(\int_0^{1} v_x^2(t,y)dy \right)^{1/2} + |v(t,x_0)| + |[v](t)| + \sqrt{|x-\sigma|} \left(\int_{\sigma}^{x} v_x^2(t,y)dy \right)^{1/2} \\ &\leq \left(\int_0^{1} v_x^2(t,y)dy \right)^{1/2} + |v(t,x_0)| + |[v](t)| + \left(\int_0^{1} v_x^2(t,y)dy \right)^{1/2} \\ &= 2\left(\int_0^{1} v_x^2(t,y)dy \right)^{1/2} + |v(t,x_0)| + |[v](t)| \end{aligned} \tag{8}$$

We now choose our x_0. First, note that

$$\frac{\partial}{\partial t} \left(\int_0^1 v(t,x)dx \right) = \int_0^1 v_t(t,x)dx = \int_0^1 v_{xx}(t,x)dx = v_x(t,1) - v_x(t,0) = 0.$$

where we have made use of the facts that v satisfies the heat equation and that there are zero input fluxes at $x = 0$ and $x = 1$. Thus $\int_0^1 v(t,x)\,dx$ is constant in time and in fact identically equal to zero (since we have $\int_0^1 v(0,x)\,dx = 0$). Since $\int_0^1 v(t,x)\,dx = 0$ at all times t, for each time t either there exists an x_0 such that $v(t,x_0) = 0$, or if no such x_0 exists, that $v(t,x) < 0$ for $x < \sigma$ and $v(t,x) > 0$ (or vice-versa).

If there exists some $x_0 \in (0,\sigma)$ such that $v(t,x_0) = 0$ (for some fixed time t) then from (7) and/or (8),

$$|v(t,x)| \leq 2\left(\int_0^{1} v_x^2(t,y)dy \right)^{1/2} + |[v](t)| \tag{9}$$

for all $x \in (0,1)$. A similar argument shows that (8) holds if there is some point x_0 in $(\sigma,1)$ with $v(t,x_0) = 0$.

However, if there is no point $x_0 \in (0,\sigma)$ or in $(\sigma,1)$ such that $v(t,x_0) = 0$ then this means that $v(t,x) < 0$ for $0 \leq x \leq \sigma$ and $v(t,x) > 0$ for $\sigma \leq x \leq 1$, or vice-versa. In this case, we can still establish inequality (9), for if without loss of generalization $v(t,x) < 0$ for $0 \leq x \leq \sigma$, then for $x \in (0,\sigma)$ we have

$$\begin{aligned} |v(t,x)| &= \left| \int_{x}^{\sigma} v_x(t,y)dy + v^-(t,\sigma) \right| \\ &\leq \sqrt{|\sigma-x|} \int_0^{1} v_x^2(t,y)dy + |[v(t)]| \end{aligned}$$

$$\leq \left(\int_0^1 v_x^2(t,y)dy\right)^{1/2} + |[v](t)|$$
$$\leq 2\left(\int_0^1 v_x^2(t,y)dy\right)^{1/2} + |[v](t)|$$

since $|v^-(t,\sigma)| < |[v](t)|$ from the given assumptions. A similar argument holds for $x \in (\sigma, 1)$. Therefore, inequality (9) is valid for all $x \in (0,1)$ at all times t.

Squaring both sides of (9) yields

$$v^2(t,x) \leq 4\int_0^1 v_x^2(t,x)dx + 4[v](t)\left(\int_0^1 v_x^2(t,y)dy\right)^{1/2} + ([v](t))^2. \tag{10}$$

From Young's inequality ($pq \leq \frac{p^2}{2\epsilon^2} + \frac{\epsilon^2 q^2}{2}$ for all ϵ) we have

$$[v(t)]\left(\int_0^1 v_x^2(t,y)dy\right)^{1/2} \leq \frac{1}{2\epsilon^2}([v](t))^2 + \frac{\epsilon^2}{2}\int_0^1 v_x^2(t,y)dy$$

for any ϵ. Inserting this into (10) we obtain

$$v^2(t,x) \leq (4+2\epsilon^2)\int_0^1 v_x^2(t,y)dy + (1+2/\epsilon^2)([v](t))^2$$

and so (after integrating both sides from $x=0$ to $x=1$ and noting that the right side is constant in terms of x)

$$\int_0^1 v^2(t,x)dx \leq (4+2\epsilon^2)\int_0^1 v_x^2(t,y)dy + (1+2/\epsilon^2)([v](t))^2$$

or with a bit of rearrangement,

$$0 \leq \int_0^1 v_x^2(t,y)dy + \frac{1+2/\epsilon^2}{4+2\epsilon^2}([v](t))^2 - \frac{1}{4+2\epsilon^2}\int_0^1 v^2(t,x)dx. \tag{11}$$

Equation (11) can be combined with equation (6) to obtain

$$\frac{\partial}{\partial t}\left(\frac{1}{2}\int_0^1 v^2(t,x)dx\right) \leq -F([v](t))[v](t) + \frac{1+2/\epsilon^2}{4+2\epsilon^2}([v](t))^2 - \frac{1}{4+2\epsilon^2}\int_0^1 v^2(t,x)dx. \tag{12}$$

To conclude the proof of Theorem 3.2 we need

Lemma 3.1 *There exists an ϵ such that*

$$-yF(y) + \frac{1+2/\epsilon^2}{4+2\epsilon^2}y^2 \leq 0$$

for all y.

Proof. Recall that one restriction on F is $-yF(y) + ky^2 \leq 0$. Thus, it is necessary to show that an ϵ exists such that the equation

$$-ky^2 + \frac{1+2/\epsilon^2}{4+2\epsilon^2}y^2 \leq 0$$

holds true. In fact, we can obtain equality by letting $\epsilon = 1/\sqrt{2k}$, and the lemma is proved.

To conclude the proof of Theorem 3.2, use the result of Lemma 3.1 in equation (12) to obtain

$$\frac{\partial}{\partial t}\left(\frac{1}{2}\int_0^1 v^2(t,x)dx\right) \leq -\frac{1}{4+2\epsilon^2}\int_0^1 v^2(t,x)dx$$

with $\epsilon = 1/\sqrt{2k}$. Letting $\phi(t) = \frac{1}{2}\int_0^1 v^2(t,x)dx$, we have $\phi'(t) \leq -\frac{1}{2+\epsilon^2}\phi(t)$ or $\phi'(t)/\phi(t) \leq -\frac{1}{2+\epsilon^2}$. Integrating from $t=0$ to $t=T$ and solving for $\phi(T)$ yields

$$\phi(T) \leq \phi(0)e^{-T/(2+\epsilon^2)} = \phi(0)e^{-2kT/(4k+1)}.$$

Of course now we have

$$\int_0^1 (u(t,x)-c)^2 dx \leq Ce^{-2kt/(4k+1)}$$

where $C = \int_0^1 v^2(0,x)dx$ is a computable quantity. The theorem has been proven.

Theorem 3.2 will allow for the future simplification of calculations by assuming zero initial conditions and will also be helpful in calculating the error in our reconstruction for the function F.

4 Complete Data for $t > 0$: Characterizing the Defect

Let use assume that $u(t,x)$ satisfies equations (1)-(5) but with $f(x) = 0$. Let us also assume that we have noiseless measurements of the endpoint temperatures at all times $t > 0$, say

$$\begin{aligned} u(t,0) &= a(t) \\ u(t,1) &= b(t) \end{aligned}$$

for some known functions $a(t)$ and $b(t)$. Under these conditions we show that the location of the defect can be uniquely determined.

From equations (2) and (3), we are given the heat fluxes at $x = 0$ and $x = 1$. In fact, we can choose these fluxes. In an attempt to be as general as possible, we will solve for the location of the defect for any boundary fluxes, as long as at least one is nonzero. Using the flux information and the endpoint temperature measurements given above, the location of σ will be recovered without knowledge of F.

Theorem 4.1 *Suppose the fluxes $g_0(t)$, $g_1(t)$ are not both identically zero. Then these fluxes and the data $a(t)$, $b(t)$ for $t > 0$ uniquely determine σ.*

Proof. To prove this, we employ the Laplace Transform, defined by

$$\mathcal{L}(h(t)) = H(s) = \int_0^\infty e^{-st}h(t)dt.$$

Then equations (1)-(5) with the zero initial conditions become

$$\begin{aligned} sU(s,x) - U_{xx}(s,x) &= 0 \text{ in } (0,\sigma)\cup(\sigma,1) \\ -U_x(s,0) &= G_0(s) \\ U_x(s,1) &= G_1(s) \\ U_x(s,\sigma) &= \mathcal{L}(F([u](t))) \end{aligned} \tag{13}$$

Equation (13) can be solved on both $(0,\sigma)$ and $(\sigma,1)$, respectively, using simple techniques in ordinary differential equations, to yield solutions of the form

$$U_L(s,x) = c_1e^{\sqrt{s}x} + c_2e^{-\sqrt{s}x} \tag{14}$$

$$U_R(s,x) = d_1e^{\sqrt{s}x} + d_2e^{-\sqrt{s}x} \tag{15}$$

where $U_L(s,x)$ denotes the Laplace transform of $u(t,x)$ with respect to t for $0 < x < \sigma$ and $U_R(s,x)$ the transform for $\sigma < x < 1$. In order to find these constants, the endpoint data measurements should be brought into the Laplace domain. Let $A(s)$ and $B(s)$ denote the Laplace transforms of $a(t)$ and $b(t)$.

The constants c_1 and c_2 in equation (14) can be found for the $(0,\sigma)$ section of Ω by solving the system of equations formed by $U_x(s,0) = G_0(s)$ and $U(s,0) = A(s)$. A similar computation can be used to find the constants d_1 and d_2 in equation (15). We find

$$\begin{aligned} U_L(s,x) &= \left(\frac{A(s)}{2} - \frac{G_0(s)}{2\sqrt{s}}\right) e^{\sqrt{s}x} + \left(\frac{A(s)}{2} + \frac{G_0(s)}{2\sqrt{s}}\right) e^{-\sqrt{s}x} \\ U_R(s,x) &= \left(\frac{B(s)}{2} + \frac{G_1(s)}{2\sqrt{s}}\right) e^{\sqrt{s}(x-1)} + \left(\frac{B(s)}{2} - \frac{G_1(s)}{2\sqrt{s}}\right) e^{-\sqrt{s}(x-1)} \end{aligned} \tag{16}$$

Since $u_x(t,x)$ is continuous across $x = \sigma$ for all time (or in this case, for all s), we set $U_{L,x}(s,\sigma) = U_{R,x}(s,\sigma)$. Using two hyperbolic trigonometric identities

$$\begin{aligned} 2\sinh(z) &= e^z - e^{-z} \\ 2\cosh(z) &= e^z + e^{-z} \end{aligned}$$

and a simple rearrangement, we get the following equation:

$$A(s)\sinh(\sqrt{s}\sigma) - \frac{G_0(s)}{\sqrt{s}}\cosh(\sqrt{s}\sigma) = B(s)\sinh(\sqrt{s}(\sigma-1)) + \frac{G_1(s)}{\sqrt{s}}\cosh(\sqrt{s}(\sigma-1)). \tag{17}$$

Applying the hyperbolic difference of angles formulas

$$\begin{aligned} \sinh(x-y) &= \sinh(x)\cosh(y) - \cosh(x)\sinh(y) \\ \cosh(x-y) &= \cosh(x)\cosh(y) - \sinh(x)\sinh(y) \end{aligned}$$

and collecting like terms, we can solve for σ uniquely:

$$\sigma = \frac{1}{\sqrt{s}}\tanh^{-1}\left(\frac{G_0(s) - B(s)\sqrt{s}\sinh(\sqrt{s}) + G_1(s)\cosh(\sqrt{s})}{A(s)\sqrt{s} - B(s)\sqrt{s}\cosh(\sqrt{s}) + G_1(s)\sinh(\sqrt{s})}\right). \tag{18}$$

Note that this must be true for each $s > 0$ (provided of course that the denominator does not vanish), so that σ is actually over-determined by the boundary data. Any nonzero value of s except for those that give rise to singularities in $G_0(s), G_1(s), A(s)$, and $B(s)$ or cause the denominator in (18) to vanish will yield the correct value for σ. Of course, in the presence of noise we expect equation (18) will not give consistent estimates of σ, an issue we address below.

We now show that the denominator on the right in equation (18) cannot vanish for all s unless $u_x(t,\sigma) \equiv 0$. We proceed by contradiction. Suppose the denominator vanishes identically in s. This implies $A(s) = B(s)\cosh(\sqrt{s}) - \frac{G_1(s)}{\sqrt{s}}\sinh(\sqrt{s})$. Plugging this value into equation (17), we find that then $G_0(s) = B(s)\sqrt{s}\sinh(\sqrt{s}) - G_1(s)\cosh(\sqrt{s})$. These two equalities, when put into equation (16), show that $U_L(s,x) = U_R(s,x)$, and hence $u^-(t,\sigma) \equiv u^+(t,\sigma)$, i.e., $[u](t) \equiv 0$. From the properties of F we conclude that $u_x(t,\sigma) \equiv 0$. In short, if $u_x(t,\sigma)$ is NOT identically zero, equation (18) must yield the correct value for σ whenever the denominator is non-zero.

However, it is possible for the denominator to vanish identically, and so equation (18) fails to yield an estimate of σ (e.g., if $\sigma = 1/2$ and $g_0(t) \equiv g_1(t)$—from symmetry we obtain $u_x(t,1/2) \equiv 0$). Nonetheless, even in this case the defect location is still uniquely determined by the flux and temperature data.

To see this, consider solutions $u_1(t,x)$ and $u_2(t,x)$ to equations (1)-(5), with defect locations σ_1 and σ_2, respectively. Assume that $\frac{\partial u_1}{\partial x}(t,\sigma_1) \equiv 0$ and $\frac{\partial u_2}{\partial x}(t,\sigma_2) \equiv 0$ (so equation (18) fails) and that

u_1 and u_2 have the same Cauchy data ($u_1(t,0) \equiv u_2(t,0)$ and both with input fluxes $g_0(t), g_1(t)$). We will show that $\sigma_1 = \sigma_2$.

Suppose, to the contrary, that $\sigma_1 \neq \sigma_2$, say $\sigma_1 < \sigma_2$. Since u_1 and u_2 have the same Cauchy data at $x = 0$ we must conclude from Theorem 3.1 that $u_1(t,x) \equiv u_2(t,x)$ for $0 \leq x \leq \sigma_1$. This implies that $\frac{\partial u_2}{\partial x}(t,\sigma_1) = \frac{\partial u_1}{\partial x}(t,\sigma_1) = 0$ for $t > 0$. Since $\frac{\partial u_2}{\partial x}(t,\sigma_2) \equiv 0$ and u_2 satisfies the heat equation for $\sigma_1 < x < \sigma_2$, we conclude that $u_2(t,x) \equiv 0$ for $\sigma_1 < x < \sigma_2$ and $t > 0$. This immediately implies that $u_2(t,x) \equiv 0$ for $0 \leq x \leq \sigma_2$ (by Theorem 3.1, since $u_2(t,\sigma_1) \equiv 0$). We are forced to conclude that $g_0(t) \equiv 0$. Similarly, since $\frac{\partial u_2}{\partial x}(t,\sigma_2) \equiv 0$ we have that $[u_2](t) \equiv 0$, forcing $u_2^+(t,\sigma_2) \equiv 0$. This, along with $\frac{\partial u_2}{\partial x}(t,\sigma_2) \equiv 0$, forces $u_2(t,x) \equiv 0$ for $\sigma_2 \leq x \leq 1$, and we conclude that $g_1(t) \equiv 0$ also, a contradiction.

This completes the proof of Theorem 4.1.

Note that although we have shown that any two distinct defects σ_1 and σ_2 must yield different endpoint data $a(t)$ and $b(t)$, we have not shown that any defect is "detectable". If $a(t)$ and $b(t)$ are the temperature measurements for a bar with defect at σ (input fluxes $g_0(t)$ and $g_1(t)$) and $a_0(t)$, $b_0(t)$ the data for a bar with no defect (same input fluxes). Then it IS possible that $a(t) \equiv a_0(t)$ and $b(t) \equiv b_0(t)$. Again, simply let $\sigma = 1/2$ with any F and $g_0(t) = g_1(t)$. Symmetry shows that the bar with defect at $\sigma = 1/2$ yields the same Cauchy data as the bar with no defect.

However, we can guarantee the "detectability" of any defect by taking, for example, $g_1(t) \equiv 0$ and any non-zero choice for $g_0(t)$. In this case the flux $u_x(t,\sigma)$ cannot vanish identically, for if so we would conclude that $u(t,x) \equiv 0$ for $\sigma < x < 1$, and hence on the entire bar, leading to the contradiction $g_0(t) \equiv 0$.

Since the identification of the defect's location has been accomplished, the focus now shifts to describing its influence on the heat flow, that is, the recovery of the function F. To do so, the problem will be converted back into the time domain.

Theorem 4.2 *The function F is uniquely determined (on the set of temperature jumps that occur) by the boundary fluxes $g_0(t)$ and $g_1(t)$, and the resulting temperature measurements at the endpoints, $a(t)$ and $b(t)$.*

Proof. Since the Laplace transform is injective, given $H(s)$, one can in principle determine $h(t)$. Thus, $U_L(s,x)$ and $U_R(s,x)$ have inverse Laplace transforms, which correspond to $u_L(t,x)$ and $u_R(t,x)$. The temperature jump at σ is defined as $[u](t) = u_R(t,\sigma) - u_L(t,\sigma)$ and the temperature flux at σ is defined as $u_{L,x}(t,\sigma) = u_{R,x}(t,\sigma)$. We can thus recover $[u](t)$ and $u_x(t,\sigma)$ for all $t > 0$, and hence we can recover $F(z)$ where z spans the range of temperature jumps which occur for $t > 0$.

This completes the proof of Theorem 4.2.

5 The Finite Time Data Version: Finding σ

So far the continuous data version, where the endpoint temperature measurements are known for all time, has been presented. This however is not practical for obvious reasons concerning the limitations and expenses of gathering temperature measurements. In sections 5-7, we are going to present the alternative, the finite-time data version of the problem, where the endpoint measurement data is sampled for the time period $(0,T)$. For practical purposes, it will be assumed that there are enough sampling points to create a negligible error in computing integrals involving $a(t)$ and $b(t)$. We will choose our endpoint fluxes as $g_0(t) = \delta(t)$ and $g_1(t) = 0$, where $\delta(t)$ is the Dirac delta function.

In this section, we compute the error in σ by making approximations for $A(s)$ and $B(s)$. From equation (18), the only error in σ introduced in the finite data version is from $A(s)$ and $B(s)$; everything else can be calculated exactly. The endpoint temperature measurements are only known for a limited time period $(0,T)$, so to approximate the Laplace transform of $a(t)$ (similarly for $b(t)$)

we use

$$A(s) = \int_0^\infty a(t)e^{-st}dt \approx \int_0^T a(t)e^{-st}dt + \int_T^\infty a_\infty e^{-st}dt$$

where a_∞ is the constant value which $u(t,x)$ approaches as $t \to \infty$. We can easily compute, as in the proof of Theorem 3.2, that $a_\infty = \int_0^R (g_0(t) + g_1(t))\,dt$, where $g_0(t)$ and $g_1(t)$ are identically zero for $t > R$. The approximation is justified based on the reasoning that the Laplace transform will have two integral components—one that is exact for the time period $(0,T)$ and one which is an estimate. The estimate is reasonable since there is a known amount of energy put into the rod, and as t becomes large, this energy becomes evenly distributed in the rod (Theorem 3.2).

This approximation will create an error ϵ_a in $A(s)$ of the following form:

$$|\epsilon_a| = \left| \int_0^\infty a(t)e^{-st}dt - \left(\int_0^T a(t)e^{-st}\,dt + \int_T^\infty a_\infty e^{-st}\,dt \right) \right| = \left| \int_T^\infty (a(t) - a_\infty)e^{-st}\,dt \right| \qquad (19)$$

Theorem 3.2) asserts that $u(t,x)$ decays to a constant value at a certain rate, as measured in the mean-square norm. We believe (but have not quite proved) that the same type of decay holds in the supremum norm, so the quantity $|a(t) - a_\infty|$ can be bounded as $|a(t) - a_\infty| \le Ce^{-\lambda t}$ where $\lambda = 2k/(4k+1)$, k as in assumption A3. In this case we can use equation (19) to obtain a bound

$$|\epsilon_a| \le \frac{C}{s} e^{-\lambda T} e^{-sT}. \qquad (20)$$

A similar error bound ϵ_b can be computed for the $B(s)$ approximation.

To find the optimal s to calculate σ (the s value providing the most accurate defect location), consider the formula for σ to be a function of $A(s)$ and $B(s)$ (all other values are exact, as stated before). Thus, to minimize the error in σ, the following equation is considered:

$$\begin{aligned} \Delta\sigma &= \frac{\partial\sigma}{\partial A}\epsilon_a + \frac{\partial\sigma}{\partial B}\epsilon_b. \\ &= \frac{-\epsilon_a + \epsilon_a B(s)\sqrt{s}\sinh(\sqrt{s}) - \epsilon_b\sqrt{s}\sinh(\sqrt{s})A(s) + \epsilon_b\cosh(\sqrt{s})}{sA^2(s) - 2sA(s)B(s)\cosh(\sqrt{s}) - 1 + 2B\sqrt{s}\sinh(\sqrt{s}) + B^2(s)s}. \end{aligned}$$

We should emphasize that this uses the assumption that $g_0(t) = \delta(t)$ and $g_1(t) \equiv 0$.

Plotting this equation and finding the value of s such that $\Delta\sigma$ is minimum (using the maximum values of ϵ_a and ϵ_b as dictated by equation (20)) yields the optimal s we use to determine σ in equation (18). Therefore, complications that arise from limited temperature measurements can be taken into quantifiable account when recovering the location of the defect.

6 The Flux Recovery

As stated previously, in order to recover F, it is necessary to know both $[u](t)$ and $u_x(t,\sigma)$. Let us make the point now that F is only recoverable for the range of jump sizes $[u](t)$ which occur during the measured time interval. For simplicity, in the remainder of the paper we will assume that $g_1(t) \equiv 0$.

From Theorem 4.2, it is possible to get the flux and jump recovery *if we are given endpoint temperature measurements for all time* by taking the inverse Laplace transform of various functions. Of course, this is impossible to do in practice. In order to get an accurate recovery of the flux and jump, Fourier series are implemented rather than inverse Laplace transforms since the error is easier to quantify.

To recover both $[u](t)$ and $u_x(t,\sigma)$, a Fourier series will be created to describe them. This will then facilitate a reasonable reconstruction of F itself, which is defined as $F([u](t)) = u_x(t,\sigma)$. The accuracy of the reconstructed F will depend on the error in the data measurements themselves and the error arising from limited data. We present an error analysis of these methods, assuming again that we have enough data to neglect integration error. This section deals solely with the flux recovery.

6.1 Recovery of $u_x(t,\sigma)$

To get a recovery for F in the manner stated before, a Fourier series is first created to describe the flux. We utilize the identity

$$\int_a^b v(0,x)u(T,x)dx + \int_0^T (v_x(T-t,b)u(t,b) - v_x(T-t,a)u(t,a))dt = \int_0^T (v(T-t,b)u_x(t,b) - v(T-t,a)u_x(t,a))dt \tag{21}$$

where u and v both satisfy the heat equation for $t > 0$, $a < x < b$, and u has zero initial conditions. This identity is easily derived through integration by parts and is included in the Appendix.

Recall that the value of σ has already been determined. To minimize error, choose (a,b) to be either $(0,\sigma)$ or $(\sigma,1)$, such that $b-a$ is minimum. Without loss of generalization, we assume $(a,b) = (0,\sigma)$.

Thus, equation (21) is transformed into, after some rearrangement

$$\int_0^T v(T-t,\sigma)u_x(t,\sigma)dt = \int_0^\sigma v(0,x)u(T,x)dx + \int_0^T v(T-t,0)g_0(t,0)dt - \int_0^T (v_x(T-t,\sigma)u(t,\sigma) + v_x(T-t,0)a(t))dt \tag{22}$$

In order to create a Fourier cosine or sine series for $u_x(t,\sigma)$, we look for test functions $v(t,x)$ which have the following properties:

P1. $v_t - v_{xx} = 0$

P2. $v(T-t,\sigma)$ takes the form of a sine or cosine

P3. $v_x(T-t,\sigma) = 0$

These properties ensure that the only terms left in the equations are computable, known quantities (in other words, the term $\int_0^T (v_x(T-t,\sigma)u(t,\sigma)$, which is not known, drops out). Also, this ensures that the Fourier coefficients for $u_x(t,\sigma)$ are indeed recoverable.

Lemma 6.1 *The functions*

$$v_1(t,x) = \frac{1}{2}e^{-\omega(x-\sigma)}\cos(2\omega^2 t - \omega(x-\sigma)) + \frac{1}{2}e^{-\omega(\sigma-x)}\cos(2\omega^2 t - \omega(\sigma-x)) \tag{23}$$

$$v_2(t,x) = \frac{1}{2}e^{-\omega(x-\sigma)}\sin(2\omega^2 t - \omega(x-\sigma)) + \frac{1}{2}e^{-\omega(\sigma-x)}\sin(2\omega^2 t - \omega(\sigma-x)) \tag{24}$$

both satisfy P1-P3.

This is easily proven by substituting v_1 and v_2 for v and checking each property P1-P3.

We make the assumption that $a(t)$ and $b(t)$ have died down to a relatively constant (as per Theorem 3.2). Furthermore, we know that this constant can be computed (with our particular input fluxes). We consider the error made by this substitution later.

Putting the test functions v_1 and v_2 into equation (22), using u_∞ for the limiting value of $u(T,x)$, and using the trigonometric identity $\sin(z)-\cos(z)=\sqrt{2}\sin(z-\frac{\pi}{4})$ yields

$$\begin{aligned}
\int_0^T u_x(t,\sigma)\cos(2\omega^2(T-t))dt &= -\frac{1}{2}\int_0^T g_0(t)(e^{\omega\sigma}\cos(2\omega^2(T-t)+\omega\sigma) \\
&+ e^{-\sigma\omega}\cos(2\omega^2(T-t)-\omega\sigma))\,dt \\
&- \frac{\sqrt{2}\omega}{2}\int_0^T a(t)(e^{\omega\sigma}\sin(2\omega(T-t)+\omega\sigma-\frac{\pi}{4}) \\
&+ e^{-\omega\sigma}\sin(2\omega^2(T-t)-\omega\sigma-\frac{\pi}{4}))dt \\
&+ u_\infty\int_0^\sigma \cos(\omega(\sigma-x))\cosh(\omega(\sigma-x))dx \qquad (25) \\
\int_0^T u_x(t,\sigma)\sin(2\omega^2(T-t))dt &= -\frac{1}{2}\int_0^T g_0(t)(e^{\omega\sigma}\sin(2\omega^2(T-t)+\omega\sigma) \\
&+ e^{-\sigma\omega}\sin(2\omega^2(T-t)-\omega\sigma))\,dt \\
&- \frac{\sqrt{2}\omega}{2}\int_0^T a(t)(e^{-\omega\sigma}\sin(2\omega(T-t)+\omega\sigma-\frac{\pi}{4}) \\
&- e^{\omega\sigma}\sin(2\omega^2(T-t)-\omega\sigma-\frac{\pi}{4}))dt \\
&+ u_\infty\int_0^\sigma \sin(\omega(\sigma-x))\sinh(\omega(\sigma-x))dx \qquad (26)
\end{aligned}$$

It is crucial to note that the right side of each of the above equations is computable. Call these $K_1(\omega)$ and $K_2(\omega)$. Expand the left hand sides of the equations to get the system of integral equations

$$\begin{aligned}
\cos(2\omega^2T)I_1(\omega)+\sin(2\omega^2T)I_2(\omega)&=K_1(\omega)\\
\sin(2\omega^2T)I_1(\omega)-\cos(2\omega^2T)I_2(\omega)&=K_2(\omega)
\end{aligned}$$

with $I_1(\omega)=\int_0^T u_x(t,\sigma)\cos(2\omega^2t)dt$ and $I_2(\omega)=\int_0^T u_x(t,\sigma)\sin(2\omega^2t)dt$. Solving this system of equations for $I_1(\omega)$ and $I_2(\omega)$ we get

$$\begin{aligned}
I_1(\omega) &= K_2(\omega)\sin(2\omega^2T)+K_1(\omega)\cos(2\omega^2T)\\
I_2(\omega) &= -K_2(\omega)\cos(2\omega^2T)+K_1(\omega)\sin(2\omega^2T)
\end{aligned}$$

To find the Fourier coefficients for $u_x(t,\sigma)$, set $\omega=\sqrt{\frac{k\pi}{2T}}$, and assume a Fourier expansion for $u_x(t,\sigma)$. In I_1, assume $u_x(t,\sigma)=\sum_{j=0}^\infty c_j\cos(\frac{j\pi t}{T})$.

Then

$$I_1(\sqrt{\frac{j\pi}{2T}})=\int_0^T\sum_{j=0}^\infty c_j\cos(\frac{j\pi t}{T})\cos(\frac{k\pi t}{T})=\sum_{j=0}^\infty\int_0^T c_j\cos(\frac{j\pi t}{T})\cos(\frac{k\pi t}{T})dt$$

Noting the orthogonality of the cosine functions on $(0,T)$ in the last integral, the Fourier cosine coefficients are computed:

$$c_j=\begin{cases}\frac{I_1(0)}{T} & : \quad j=0\\ \frac{2I_1(\sqrt{\frac{j\pi}{2T}})}{T} & : \quad j\neq 0\end{cases}$$

To reiterate, $u_x(t,\sigma)=\sum_{j=0}^\infty c_j\cos(\frac{j\pi t}{T})$. Finding the Fourier sine coefficients is done in a similar fashion using I_2. Thus, we have found a Fourier sine and cosine reconstruction for $u_x(t,\sigma)$.

As stated before, these reconstructions are not exact. There are two sources of error in this analysis. First, we assumed in equation (22) that $u(T,x)$ is constant. But with limited data, with time only from $t=0$ to $t=T$, there will be some discrepancy between $u(T,x)$ and u_∞, its limiting value in T. Second, error in the reconstruction will appear if the instrument measuring the endpoint temperature measurements has error (in other words, if there is some "noise" in $a(t)$ and $b(t)$). Both of these errors will be addressed separately in subsections 6.2 and 6.3.

6.2 Error from Limited Data

In this section we derive a simple error bound on c_j, the Fourier cosine coefficients, due to the truncation of the data at time T. Although the bound is far from sharp, it does illustrate that as T gets larger we can expect the estimate of c_j go become more accurate.

In equation (22), we replace $\int_0^\sigma v(0,x)u(T,x)dx$ with the approximation $u_\infty \int_0^\sigma v(0,x)dx$ giving an error of

$$\left| \int_0^\sigma (u(T,x)-u_\infty)v(0,x)dx \right|.$$

Applying Hölder's Inequality to this error yields

$$\begin{aligned}
|\text{Error in } K_1, K_2| &= \left| \int_0^\sigma (u(T,x)-u_\infty)v(0,x)dx \right| \\
&\leq \left(\int_0^\sigma (u(T,x)-u_\infty)^2)dx \right)^{1/2} \left(\int_0^\sigma v^2(0,x)dx \right)^{1/2} \\
&\leq \left(\int_0^1 (u(T,x)-u_\infty)^2)dx \right)^{1/2} \left(\int_0^\sigma v^2(0,x)dx \right)^{1/2} \\
&\leq Ce^{\frac{-2kT}{4k+1}} \left(\int_0^\sigma v^2(0,x)dx \right)^{1/2}
\end{aligned}$$

where C is a constant and the last inequality is derived from Theorem 3.2.

Using the test functions v_1 and v_2 defined in equations (23) and (24), and taking the "worst case" for the integral (making it as large as possible), we get

$$|\text{Error in } K_1(\omega),\, K_2(\omega)| \leq Ce^{\frac{-2kT}{4k+1}} \sqrt{\frac{1}{32\omega}(6+8\omega\sigma+4e^{2\omega\sigma})}.$$

From this, the maximum error bounds in $K_1(\omega)$ and $K_2(\omega)$ are found to be the above values, which gives the maximum error bound in $I_1(\omega)$ (a similar computation for $I_2(\omega)$ can be made) to be

$$|\text{Error in } I_1(\omega)| \leq Ce^{\frac{-2kT}{4k+1}} \sqrt{\frac{1}{32\omega}(6+8\omega\sigma+4e^{2\omega\sigma})}.$$

With $\omega = \sqrt{\frac{j\pi}{2T}}$, this error becomes

$$|\text{Error in } I_1(\sqrt{\tfrac{j\pi}{2T}})| \leq Ce^{\frac{-2kT}{4k+1}} \sqrt{\frac{\sqrt{2T}}{32\sqrt{j\pi}}(6+8\sigma\sqrt{\frac{j\pi}{2T}}+4e^{2\sqrt{\frac{j\pi}{2T}}\sigma})}.$$

Remembering that the Fourier coefficients are defined by $c_j = \frac{2I_1}{T}$ for $j \neq 0$, we find

$$\begin{aligned}
|\text{Error in } c_j| &\leq \frac{2}{T}Ce^{\frac{-2kT}{4k+1}} \sqrt{\frac{\sqrt{2T}}{32\sqrt{j\pi}}(6+8\sigma\sqrt{\frac{j\pi}{2T}}+4e^{2\sqrt{\frac{j\pi}{2T}}\sigma})} \\
&\leq \frac{D\sqrt{\alpha+\beta\sqrt{j}+\gamma e^{\delta\sqrt{j}}}}{j^{1/4}} \qquad (27)
\end{aligned}$$

for $D, \alpha, \beta, \gamma, \delta$ are all constants. Note that as $T \to \infty$ the error in c_j (for any fixed j) approaches zero.

A simple calculation reveals that the error for c_0 is bounded by $\frac{Ce^{-\frac{2kT}{4k+1}}}{T}$

6.3 Error from Noise

The instruments used to measure the temperature at $x = 0$ and $x = 1$ are only accurate to a certain degree. Error in these measurements will affect the recovery of the flux and thus the later reconstruction of the function F. We will now compute the error in each Fourier coefficient that comes from this noise.

Let $a(t) = \tilde{a}(t) + \epsilon(t)$ be the temperature measurements at the $x = 0$, where $\tilde{a}(t)$ is the true temperature and $\epsilon(t)$ is the error in this measurement. The error this causes in $K_1(\omega)$ and $K_2(\omega)$ are respectively

$$\frac{\sqrt{2}\omega}{2}e^{\omega\sigma}\int_0^T \epsilon(t)\sin(2\omega^2(T-t)+\omega\sigma-\frac{\pi}{4})dt + \frac{\sqrt{2}\omega}{2}e^{-\omega\sigma}\int_0^T \epsilon(t)\sin(2\omega^2(T-t)-\omega\sigma-\frac{\pi}{4})dt$$
$$\frac{\sqrt{2}\omega}{2}e^{\omega\sigma}\int_0^T \epsilon(t)\cos(2\omega^2(T-t)+\omega\sigma-\frac{\pi}{4})dt + \frac{\sqrt{2}\omega}{2}e^{-\omega\sigma}\int_0^T \epsilon(t)\cos(2\omega^2(T-t)-\omega\sigma-\frac{\pi}{4})dt.$$

This can be seen from equations (25) and (26). We bound this error by bounding the integrals by the maximum value possible. Thus,

$$|\text{Error in } K_1(\omega),\, K_2(\omega)| \le \frac{\sqrt{2}\omega}{2}e^{\omega\sigma}(T|\epsilon(t)|_\infty) + \frac{\sqrt{2}\omega}{2}e^{-\omega\sigma}(T|\epsilon(t)|_\infty) = \sqrt{2}\omega T|\epsilon(t)|_\infty\cosh(\omega\sigma)$$

where $|\epsilon(t)|_\infty$ is the maximum value of $|\epsilon(t)|$. This value can be computed in various ways. If, for example, the instrument measuring the endpoint temperature has an absolute maximum error, then that would be the value of $|\epsilon(t)|_\infty$. If the error in the reading is some percentage of the value of the temperature, then $|\epsilon(t)|_\infty$ will be the maximum temperature reading multiplied by this percentage.

The error in $I_1(\omega)$ (error in $I_2(\omega)$ can be computed similarly) after letting $\omega = \sqrt{\frac{j\pi}{2T}}$ is

$$|\text{Error in } I_1(\sqrt{\tfrac{j\pi}{2T}})| \le \sqrt{j\pi T}|\epsilon(t)|_\infty\cosh(\sqrt{\frac{j\pi}{2T}}\sigma).$$

Again, since $c_j = \frac{2I_1}{T}$ for $j \neq 0$, we find

$$|\text{Error in } c_j| \le 2\sqrt{\frac{j\pi}{T}}|\epsilon(t)|_\infty\cosh(\sqrt{\frac{j\pi}{2T}}\sigma). \tag{28}$$

Equation (28) illustrates that the difficulty of recovering the higher Fourier coefficients of $u_x(t, \sigma)$ increases exponentially with frequency j and with defect depth σ. We thus expect some kind of regularization to be required in the presence of any significant noise.

7 The Temperature Jump Recovery

A similar process is done to reconstruct $[u](t)$ as a Fourier series. The same two types of error, arising from limited data and noise in the data, will also be considered.

7.1 Recovery of $[u](t)$

Substituting $(a,b) = (0,\sigma)$ and $(a,b) = (\sigma,1)$ into equation (21), adding the resulting equations, inserting known values, and rearranging, yields

$$\begin{aligned}\int_0^T [u](t)v_x(T-t,\sigma)dt &= \int_0^\sigma v(0,x)u^-(T,x)dx + \int_\sigma^1 v(0,x)u^+(T,x)dx \\ &- \int_0^T (g_0(t)v(T-t,0))dt - \int_0^T (a(t)v_x(T-t,0) - b(t)v_x(T-t,1))dt\end{aligned}$$

where we have taken $g_1(t) \equiv 0$. As in the previous section, the substitution $u(T,x) = u_\infty$ is made. An error analysis to see how this substitution affects the resulting Fourier coefficients is presented in subsection 7.2.

The substitution transforms the above equation into

$$\begin{aligned}\int_0^T [u](t)v_x(T-t,\sigma)dt &= u_\infty \int_0^1 v(0,x)dx - \int_0^T (g_0(t)v(T-t,0))dt \\ &- \int_0^T (a(t)v_x(T-t,0) - b(t)v_x(T-t,1))dt \qquad (29)\end{aligned}$$

As in the flux recovery, we must find test functions $v(t,x)$ which satisfy

P1. $v_t - v_{xx} = 0$

P2. $v_x(T-t,\sigma)$ takes the form of a sine or cosine.

These properties allow for the recovery of a Fourier series for $[u](t)$ since the right hand side of equation (29) can be computed exactly.

Lemma 7.1 *The functions*

$$v_1(t,x) = e^{-\omega x}\cos(2\omega^2 t - \omega x) \qquad (30)$$

$$v_2(t,x) = e^{-\omega x}\sin(2\omega^2 t - \omega x) \qquad (31)$$

both satisfy P1 and P2.

This is easily shown by substituting v_1 and v_2 for v and checking P1 and P2.

Put v_1 and v_2 into equation (29), denote the right sides by $K_1(\omega)$ and $K_2(\omega)$ respectively, and use the trigonometric identity $\sin(z) - \cos(z) = \sqrt{2}\sin(z - \frac{\pi}{4})$, to get

$$\sqrt{2}\omega e^{-\omega\sigma}\int_0^T [u](t)\sin(2\omega^2(T-t) - \omega\sigma - \frac{\pi}{4})dt = K_1(\omega) \qquad (32)$$

$$-\sqrt{2}\omega e^{-\omega\sigma}\int_0^T [u](t)\sin(2\omega^2(T-t) - \omega\sigma + \frac{\pi}{4})dt = K_2(\omega) \qquad (33)$$

We use simple trigonometric identities to get

$$\begin{aligned}\cos(\xi_1)I_1(\omega) - \sin(\xi_1)I_2(\omega) &= \frac{-K_1(\omega)e^{\omega\sigma}}{\omega\sqrt{2}} \\ \cos(\xi_2)I_1(\omega) - \sin(\xi_2)I_2(\omega) &= \frac{K_2(\omega)e\omega\sigma}{\omega\sqrt{2}}\end{aligned}$$

where $\xi_1 = 2\omega^2 T - \omega\sigma - \frac{\pi}{4}$, $\xi_2 = 2\omega^2 T - \omega\sigma + \frac{\pi}{4}$, $I_1(\omega) = \int_0^T [u](t)\sin(2\omega^2 t)dt$, and $I_2(\omega) = \int_0^T [u](t)\cos(2\omega^2 t)dt$. Solving this system of equations for $I_1(\omega)$ and $I_2(\omega)$,

$$I_1(\omega) = -\frac{\sqrt{2}e^{\omega\sigma}}{2\omega}(\sin(\xi_1)K_2(\omega) + \sin(\xi_2)K_1(\omega))$$

$$I_2(\omega) = -\frac{\sqrt{2}e^{\omega\sigma}}{2\omega}(\cos(\xi_1)K_2(\omega) + \cos(\xi_2)K_1(\omega))$$

Examining $I_1(\omega)$ with $\omega = \sqrt{\frac{j\pi}{2T}}$ and a Fourier sine representation for the jump $[u](t) = \sum_{j=1}^{\infty} c_j \sin(\frac{j\pi t}{T})$,

$$I_1(\sqrt{\frac{j\pi t}{T}}) = \int_0^T \sum_{j=1}^{\infty} c_k \sin(\frac{j\pi t}{T}) \sin(\frac{k\pi t}{T})dt = \sum_{j=1}^{\infty} \int_0^T c_k \sin(\frac{j\pi t}{T}) \sin(\frac{k\pi t}{T})dt$$

As in the flux reconstruction, the last integral contains orthogonal functions. Thus, the Fourier coefficients are

$$c_j \quad = \quad \frac{2I_1(\sqrt{\frac{j\pi}{2T}})}{T},$$

and a reconstruction for the jump is $[u](t) = \sum_{j=1}^{\infty} c_j \sin(\frac{j\pi t}{T})$.

7.2 Error from Limited Data

In equation (29) we replaced $\int_0^1 v(0,x)u(T,x)dx$ with the approximation $\int_0^1 v(0,x)dx$ giving an error of

$$\left| \int_0^1 (u(T,x) - u_\infty)v(0,x)dx \right|.$$

Applying Hölder's inequality, we get

$$\begin{aligned} |\text{Error in } K_1, K_2| &= \left| \int_0^1 (u(T,x) - u_\infty)v(0,x)dx \right| \\ &\leq \left(\int_0^1 (u(T,x) - u_\infty)^2 dx \right)^{1/2} \left(\int_0^1 v^2(0,x)dx \right)^{1/2} \\ &\leq Ce^{-\frac{2kT}{4k+1}} \left(\int_0^1 v^2(0,x)dx \right)^{1/2} \end{aligned}$$

where C is a constant and the second inequality is derived from Theorem 3.2.

Using the test functions v_1 and v_2 defined in equations (30) and (31), and taking the "worst case" for the integral (making it as large as possible), we get

$$|\text{Error in } K_1(\omega)| \leq Ce^{-\frac{2kT}{4k+1}} \sqrt{\frac{5}{8\omega}}$$

for v_1 and

$$|\text{Error in } K_2(\omega)| \leq Ce^{-\frac{2kT}{4k+1}} \sqrt{\frac{3}{8\omega}}$$

for v_2.

These equations give us a bound for the error made by the substitution. From this, the error in $I_1(\omega)$ (a similar computation for $I_2(\omega)$ can be made) is

$$\begin{aligned} |\text{Error in } I_1(\omega)| &\leq \frac{\sqrt{2}}{2}e^{\omega\sigma}(Ce^{-\frac{2kT}{4k+1}} \sqrt{\frac{3}{8\omega}} \sin(2\omega^2 T - \omega\sigma - \frac{\pi}{4}) + Ce^{-\frac{2kT}{4k+1}} \sqrt{\frac{5}{8\omega}} \sin(2\omega^2 T - \omega\sigma - \frac{\pi}{4})) \\ &\leq \frac{\sqrt{2}}{2}e^{\omega\sigma}Ce^{-\frac{2kT}{4k+1}} \left(\frac{\sqrt{3}+\sqrt{5}}{\sqrt{8\omega}} \right). \end{aligned}$$

Letting $\omega = \sqrt{\frac{j\pi}{2T}}$, this error becomes

$$|\text{Error in } I_1(\sqrt{\tfrac{j\pi}{2T}})| \leq \frac{C(\sqrt{3}+\sqrt{5})}{2^{7/8}\pi^{1/4}} \frac{e^{\sqrt{\frac{j\pi}{2T}}\sigma - \frac{2kT}{4k+1}} T^{1/4}}{j^{1/4}}$$

Now remembering that $c_j = \frac{2I_1}{T}$, we have

$$\begin{aligned} |\text{Error in } c_j| &\leq \frac{C(\sqrt{3}+\sqrt{5})}{2^{3/4}\pi^{1/4}} \frac{e^{\sqrt{\frac{j\pi}{2T}} - \frac{2kT}{4k+1}}}{T^{3/4} j^{1/4}} \\ &\leq \frac{D e^{\alpha\sqrt{j}-\beta}}{j^{1/4}} \end{aligned} \tag{34}$$

for constants D, α, β.

7.3 Error from Noise

As in the flux recovery, the impact from the error in the instruments which gather the temperature measurements needs to be assessed. As before, let $a(t) = \tilde{a}(t) + \epsilon(t)$ be the temperature measurements at $x = 0$, where $\tilde{a}(t)$ is the true temperature and $\epsilon(t)$ is the error in this measurement. The error this causes in $K_1(\omega)$ and $K_2(\omega)$ are respectively:

$$\begin{aligned} \omega \int_0^T \epsilon(t)(\cos(2\omega^2(T-t)) - \sin(2\omega^2(T-t)))\, dt, \\ -\omega \int_0^T \epsilon(t)(\cos(2\omega^2(T-t)) + \sin(2\omega^2(T-t)))\, dt \end{aligned}$$

Both integrals are easily bounded to yield

$$|\text{Error in } K_1(\omega), K_2(\omega)| \leq 2\omega |\epsilon(t)|_\infty$$

where $|\epsilon(t)|_\infty$ is the supremum of $\epsilon(t)$ on $(0, T)$. This yields an error bound on $I_1(\omega)$ (and a bound on $I_2(\omega)$ is similar) of

$$|\text{Error in } I_1(\omega)| \leq C e^{\omega\sigma} |\epsilon(t)|_\infty$$

for some constant C. Since $c_j = \frac{2I_1}{T}$ and $\omega = \sqrt{\frac{j\pi}{2T}}$ we find an error bound of the form

$$|\text{Error in } c_j| \leq C |\epsilon(t)|_\infty e^{\sqrt{\frac{j\pi}{2T}}\sigma} \tag{35}$$

for some constant C. As with the flux, we expect high frequencies (large j) to be difficult to recover, and the difficulty increases exponentially with defect depth σ.

8 Ill-Posedness and Examples

We have found bounds for various errors in the Fourier coefficients of the flux and jump reconstructions. All these bounds show the magnitude of error in c_j increases as j increases. So for sufficiently large j, c_j contains little information about the true Fourier coefficient; the coefficient has been greatly corrupted by noise. This is the *ill-posedness* of the inverse problem – certain high frequency detail information about the flux and jump are lost to noise. To mitigate this phenomenon, we cut off higher, more corrupted, modes of the Fourier expansion:

$$u_x(t, \sigma) \approx \sum_{j=0}^{N} c_j \cos(\frac{j\pi t}{T})$$

$$[u](t) \approx \sum_{j=1}^{N} c_j \sin(\frac{j\pi t}{T})$$

How does one pick an appropriate N? It is known that Fourier coefficients must die down to zero as j gets large. Error will instead force Fourier coefficients to increase in magnitude as j gets large (see, for example, equations (28) and (35)). So by inspection, one can pick an N where the Fourier coefficients appear to stop converging to zero. This is one method for reducing noise in the reconstruction. In addition, all the bounds we found show that for large T, error is reduced. This makes sense – the more data collected, the better the reconstruction.

To illustrate this, and show how a reconstruction is possible by this method, we gather four sets of simulated endpoint temperature data. The data were generated computationally, by reducing the problem (1)-(5) to a system of four integrals equations, then solving the integrals equations with a simple fixed-point iteration scheme (see [1]). The solutions are accurate to about 4 significant figures.

The first set has data collected for 1 second, the second for 2 seconds, the third for 3 seconds, and the fourth for 4 seconds. Each set of data was generated using

$$\begin{aligned} \sigma &= 0.25 \\ F(x) &= 0.8x + 3x^3 \\ g_0(t) &= \begin{cases} 4 & \text{for} \quad t \leq 0.25 \\ 0 & \text{for} \quad t > 0.25 \end{cases} \\ g_1(t) &= 0. \end{aligned}$$

We collected, for each set of data, 100 Fourier coefficients for both the flux and jump reconstructions.

Figure 1 illustrates the flux reconstruction using one and four seconds worth of data, respectively. Not surprisingly, the four second reconstruction is considerably more stable. Figure 2 illustrates the jump reconstruction using one and four seconds worth of data, respectively. Again, the four second reconstruction is considerably more stable.

We now include reconstructions of the function F, in order to demonstrate that a recovery is possible by these methods. Since $u_x(t, \sigma) = F([u](t))$, we show below a plot of $u_x(t, \sigma)$ versus $[u](t)$, which should approximate the graph of F. Figure 3 illustrates this reconstruction using varying amounts of data. Of course for each graph in Figure 3 the "shaky" lines are the reconstructions of F, and the smooth curve is the true graph of F. Not surprisingly, the more data there is, the closer the reconstruction is to the true value.

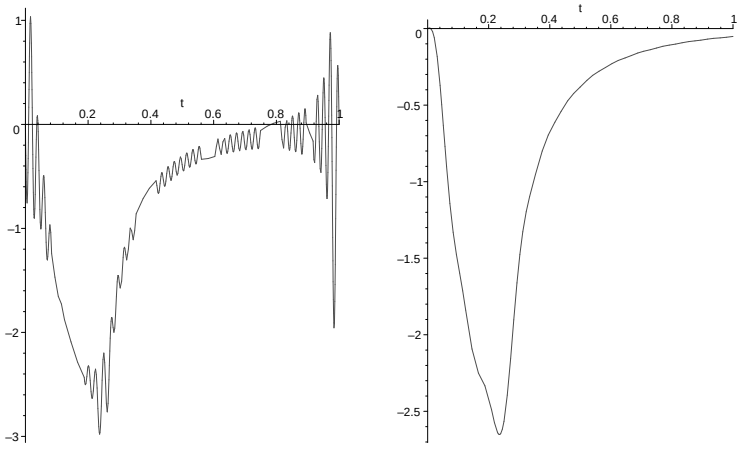

Flux Reconstruction, 1 Second Flux Reconstruction, 4 Seconds

Figure 1

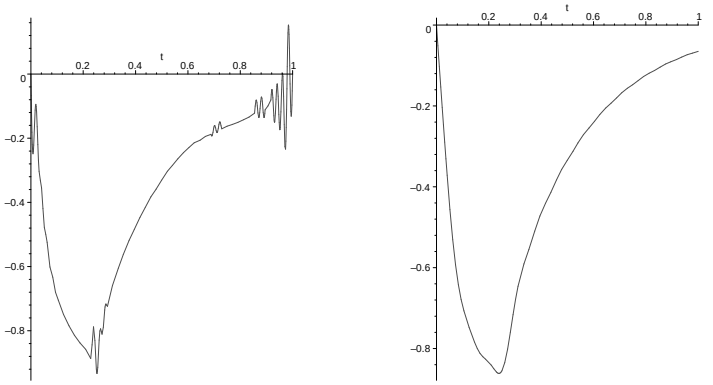

Jump Reconstruction, 1 Second Jump Reconstruction, 4 Seconds

Figure 2

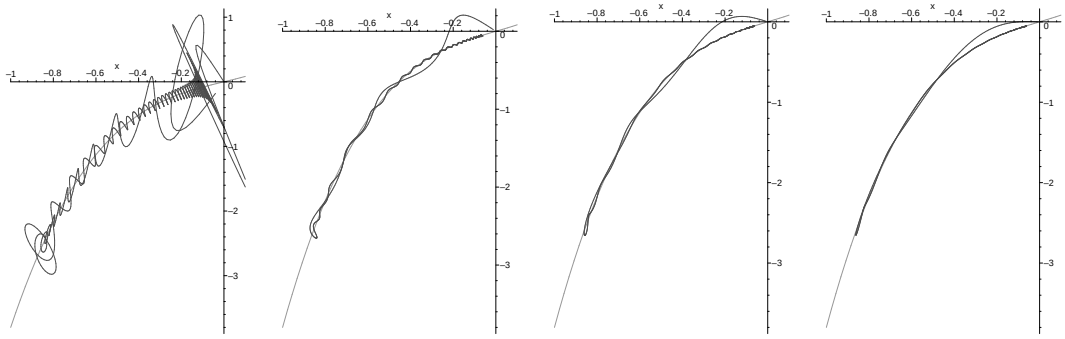

1 Second 2 Seconds 2 Seconds 1 Second

Figure 3

9 Conclusion

The research presented in this paper demonstrates that both the location and governing boundary conditions of a defect in the interior of a one-dimensional rod can be extracted from the boundary temperature response to a heat flux introduced at the boundaries. This was accomplished by using boundary measurements to first recover the defect location σ, then reconstruct both the flux $u_x(t, \sigma)$ and jump $[u](t)$ at the defect through the use of Laplace transforms, carefully chosen "test functions" in integration by parts, and Fourier series representations. We are also able to provide useful error bounds on our estimates, by analyzing the rate of decay of solutions to the forward problem (to bound error from finite-time or truncated data) and by analyzing the test function properties to bound the error introduced by noise in the data.

Further refinements to this approach would include a more coherent strategy for choosing the value of s in equation (18) or better yet, combining estimates based on many choices of s, with a more thorough understanding how the estimate may vary with varying s (and noisy data). We also have not yet implemented any regularization strategy for the reconstruction, an essential step if the data contains significant noise. However, the analysis of how the noise affects the reconstruction should be of value in devising a regularization scheme.

We hope our research can set precedence for future work in the use of thermal imaging for characterizing a defect in an object. We would especially like to extend these results to two or three

space dimensions, the imaging of multiple defects, and perhaps more general boundary conditions at the defect interface.

Appendix

We now present the derivation of Equation (21).

Consider the heat equation on some interval $a < x < b$, with $t > 0$ and zero initial conditions. Since $u_t - u_{xx} = 0$,

$$w(t,x)(u_t(t,x) - u_{xx}(t,x)) = 0$$

for any function $w(t,x)$. Integrating both sides of the equation from along the interval and for some length of time, and breaking the equation into two,

$$\int_a^b \int_0^T w(t,x)u_t(t,x) - \int_0^T \int_a^b w(t,x)u_{xx}(t,x)dxdt \quad = \quad 0 \tag{36}$$

Integrating the first piece above by parts in t to find

$$\int_a^b \int_0^T w(t,x)u_t(t,x)dtdx = \int_a^b w(T,x)u(T,x) - \int_a^b \int_0^T w_t(t,x)u(t,x)dtdx. \tag{37}$$

Now consider the second integral in (36). Integrate it by parts in x:

$$\int_0^T \int_a^b w(t,x)u_{xx}(t,x)dxdt = \int_0^T (w(t,b)u_x(t,b) - w(t,a)u_x(t,a))dt - \int_0^T \int_a^b w_x(t,x)u_x(t,x)dxdt.$$

Again, use integration by parts on the second integral above to obtain

$$\begin{aligned} \int_0^T \int_a^b w(t,x)u_{xx}(t,x)dxdt \quad = \quad & \int_0^T (w(t,b)u_x(t,b) - w(t,a)u_x(t,a))dt \\ & - \int_0^T (w_x(t,b)u(t,b) - w_x(t,a)u(t,b) - w_x(t,a)u(t,a))dt \\ & + \int_0^T \int_a^b w_{xx}(t,x)u(t,x)dxdt \end{aligned} \tag{38}$$

Using the right side of equation (37) to replace the first integral in (36), and the right side of equation (38) to replace the second integral in (36), and rearranging

$$\begin{aligned} & \int_0^T (w_x(t,b)u(t,b) - w_x(t,a)u(t,a))dt - \int_0^T (w(t,b)u_x(t,b) - w(t,a)u_x(t,a))dt \\ & - \int_0^T \int_a^b (w_t(t,x) + w_{xx}(t,x))u(t,x)dxdt + \int_a^b w(T,x)u(T,x)dx = 0 \end{aligned}$$

We now, to simplify this equation, put the constraint on w that it must satisfy the *backwards* heat equation $w_t + w_{xx} = 0$. It is easily checked that if $w(t,x) = v(T-t,x)$, then v satisfies the forward heat equation. From this we derive equation (21):

$$\begin{aligned} \int_a^b v(0,x)u(T,x)dx + & \int_0^T (v_x(T-t,b)u(t,b) - v_x(T-t,a)u(t,a))dt \\ & = \int_0^T (v(T-t,t)u_x(t,b) - v(T-t,a)u_x(t,a))dt \end{aligned}$$

References

[1] Bryan, K. and Caudill, L. *Solvability of a Parabolic Boundary Value Problem with Internal Jump Condition*, Rose-Hulman Mathematics Technical Report MS 00-04, 2000.

[2] Cannon, J.R., "The One-Dimensional Heat Equation", Addison-Wesley, 1984.